MICROMECHANICAL ANALYSIS OF THE ELASTIC BEHAVIOR OF RANDOM DISTRIBUTED FIBER REINFORCED CONCRETE

Vanessa Fátima Pasa
Alexandre Rodrigues Pacheco
Américo Campos Filho
Samir Maghous
vanessapasa@gmail.com
apacheco@ufrgs.br
americo@ufrgs.br
samir.maghous@ufrgs.br
Programa de Pós-Graduação em Engenharia Civil, Universidade Federal do Rio Grande do Sul
Av. Osvaldo Aranha, 99, 3º. Andar, 90035-190, Porto Alegre – RS – Brasil

Abstract. *Fiber reinforced concrete falls within the general category of cement-based matrix composites, whose mechanical properties are improved by the insertion of short fibers. In the perspective of a wide use in structural engineering, a comprehensive formulation of the corresponding behavior is necessary. In this context, the present paper describes a micromechanical model for the macroscopic elastic properties of fiber reinforced concrete. Reasoning on the representative elementary volume (REV) of such a composite, the overall elastic characteristics are determined from the knowledge of the elastic properties of its constituents, i.e., matrix and fibers. Modeling the fibers as prolate inclusions embedded within the concrete matrix, the Mori-Tanaka scheme is used to derive estimates of the elastic coefficients. The impact of some reinforcement parameters, such as stiffness or volume fraction of fibers, on the macroscopic scale is analyzed. Finally, the accuracy of the micromechanical predictions is assessed by comparison with finite element solutions.*

Keywords: *Concrete, Fibers, Micromechanics, Elasticity*

1. INTRODUCTION

New materials have continuously been developed according to the necessity of both reducing deficiencies and increasing the performances of materials already available. In this context, fiber reinforced concrete (FRC), although being a material of a fairly recent usage, has been showing a promising potential for structural use.

FRC is currently used in a wide range of applications, including bridge decks, airport pavements, tunnels and others. FRC is a composite material formed by a cement matrix and a quantity of dispersed fibers, resulting in a compound of improved properties. Studies have indicated that the addition of fibers improve the performance of concrete and minimize its typical fragile behavior (Figueiredo, 2005). Moreover, the addition of short fibers in the cement matrix improves its post-cracking behavior (ductility, performance under dynamic loading and cracking control) and can also alter tensile strength (Furlan and Hanai, 1997). In general, the character and performance of fiber reinforced concrete changes with varying concrete composition as well as the fiber material type, fiber geometry, fiber distribution, fiber orientation and fiber concentration (Zollo, 1997).

The design, analysis and numerical simulations of structures involving fiber reinforced concrete depend on the ability to evaluate mechanical characteristics and constitutive equations. A traditional way to formulate constitutive models is based on empirical procedures established experimentally. The main disadvantage of this approach, however, is the limitation of experimental results by the conditions to which the tests are usually bounded. Moreover, new materials and their applications tend to require both extensive and costly experimental programs for complete characterization of the constitutive behaviors.

An alternative method, which is adopted in this study, consists in reasoning to the homogenization techniques of random media. It is sought through this approach to describe the macroscopic mechanical behavior of composite materials by implementing an upscaling technique. The final objective is the replacement of a heterogeneous media, in this case the fiber reinforced concrete, by an equivalent homogeneous media, whose constitutive equations in elasticity result from the resolution of a boundary problem over the representative elementary volume (REV).

Several micromechanical models have been developed to estimate the elastic properties of different composite materials. They are mostly based on the result established by Eshelby (1957) and related to ellipsoidal inclusions embedded within the infinite medium. Depending on the morphology of the microstructure, estimation schemes of elastic properties of the composites may refer to the diluted estimation (Russel, 1973), Mori-Tanaka (Jiang et al., 2007; Chou et al., 1980; Hashin, 1968), self-consistent (Benveniste, 1987; Chen and Cheng, 1996) or generalized self-consistent (Christensen, 1979). In the present study the Mori–Tanaka scheme is used to determine the elastic properties of the fiber reinforced concrete. A study aimed at evaluating the impact of different parameters of reinforcement, such as stiffness, geometry, and volume fraction of fibers on the overall behavior of composite material was done.

Finally, the results obtained through micromechanical predictions are compared with those obtained by examining the same issue through the finite element method.

2. MACROSCOPIC ELASTIC PROPERTIES

The equivalent inclusion method (EIM) was adopted to analyze the elastic properties of fiber reinforced concrete. Concrete is idealized as a homogeneous matrix and the fibers are treated as randomly distributed and randomly oriented inhomogeneities within the matrix. The

homogeneity assumed for the concrete matrix can result of a preliminary homogenization process, which accounts for possible microcracks.

2.1 The equivalent inclusion method (EIM)

Let us consider a medium occupying a geometric domain D, made up of a homogeneous elastic matrix surrounding an elastic inhomogeneity (Fig. 1). The sub-domains occupied by the inhomogeneity and the matrix are respectively Ω e D-Ω. The elastic properties of the matrix and the inhomogeneity are characterized by their elastic moduli, C^0_{ijmn} and C^I_{ijmn}, respectively.

The loading of system D is defined by a homogenous stress $\underline{\underline{\sigma}}^0.\underline{n}$ applied on the boundary ∂D of domain D. The vector $\underline{n}$ denotes the outer normal to ∂D.

In the absence of inhomogeneity Ω, the loading defined by $\underline{\underline{\sigma}}^0$ induces in the matrix D a uniform distribution of strain $\underline{\underline{\varepsilon}}^0$, such that $\sigma^0_{ij} = C^0_{ijmn}\varepsilon^0_{mn}$. In contrast, the presence of the inhomogeneity causes stress disturbances in both constituents. The Hooke's Law may be written in average form as

$$\sigma^0_{ij} + \bar{\sigma}^0_{ij} = C^0_{ijmn}(\varepsilon^0_{mn} + \bar{\varepsilon}^0_{mn}) \text{ in D-}\Omega \qquad \text{and} \qquad \sigma^0_{ij} + \bar{\sigma}^I_{ij} = C^I_{ijmn}(\varepsilon^0_{mn} + \bar{\varepsilon}^I_{mn}) \text{ in } \Omega. \qquad (1)$$

where $\bar{\sigma}^0_{ij}$ and $\bar{\sigma}^I_{ij}$ are the average stress disturbances in the matrix and the inclusion, and $\bar{\varepsilon}^0_{mn}$ and $\bar{\varepsilon}^I_{mn}$ are the corresponding average strain disturbances, respectively.

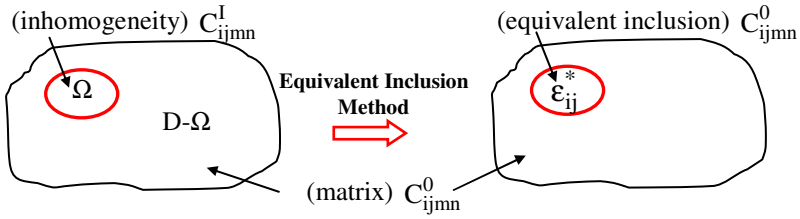


Figure 1- Scheme representation of the Equivalent Inclusion Method (Teng et al., 2004).

The basic concept of the EIM consists in replacing the inhomogeneity by an equivalent inclusion having the same elastic properties than the matrix and submitted to an initial fictitious eigenstrain ε^*_{ij} (Fig. 1). Accordingly, the right-hand equation (1) can be rewritten as follows:

$$\sigma^0_{ij} + \bar{\sigma}^I_{ij} = C^0_{ijmn}(\varepsilon^0_{mn} + \bar{\varepsilon}^I_{mn} - \varepsilon^*_{mn}) \text{ in } \Omega. \qquad (2)$$

Eshelby (1957) demonstrated that if D is infinite and Ω has ellipsoidal shape, then the strain of the inclusion is homogeneous, i.e., $\varepsilon^I_{mn} = \bar{\varepsilon}^I_{mn}$. Moreover, $\bar{\varepsilon}^I_{mn}$ is related to ε^*_{mn} through the so-called Eshelby tensor S_{ijkl}

$$\bar{\varepsilon}_{ij}^{I} = S_{ijkl}\varepsilon_{kl}^{*}. \tag{3}$$

Close-form expressions of the Eshelby tensor derived for a particular configuration can be found, for instance, in Mura (1982). This tensor is a function only of the shape and orientation of the inclusion (fiber) and the elastic properties of the matrix.

From Equations (1), (2) and (3), it can be finally found the following relationship between the strain of the inclusion, ε_{ij}^{I}, and the homogeneous strain of the boundary, ε_{kl}^{0}:

$$\varepsilon_{ij}^{I} = A_{ijkl}\varepsilon_{kl}^{0}. \tag{4}$$

where A_{ijkl} is the concentration tensor of strains and can be written as

$$A_{ijkl} = \left[I_{ijkl} + P_{ijpq}^{0,I}\left(C_{pqkl}^{I} - C_{pqkl}^{0}\right)\right]^{-1}. \tag{5}$$

I_{ijkl} is the fourth order identity tensor and $P_{ijpq}^{0,I}$ the Hill tensor:

$$I_{ijkl} = \frac{1}{2}\left(\delta_{ik}\delta_{jl} + \delta_{il}\delta_{jk}\right) \qquad \text{and} \qquad P_{ijpq}^{0,I} = S_{ijmn}\left[C_{mnpq}^{0}\right]^{-1}. \tag{6}$$

It should be recalled that Eshelby's result assumes that the inhomogeneity has an ellipsoidal shape. This result is applied herein to the situation of fibers embedded in a concrete matrix, where each fiber is represented by an ellipsoid elongated in the direction of its poles (prolate ellipsoid).

Owing to the assumption of elastic isotropy of both constituents and random distribution of the fibers, fiber reinforced concrete has, on the macroscopic scale, isotropic elastic properties.

2.2 The Mori-Tanaka Scheme

Based on the EIM and the Eshelby solution (1957), Mori-Tanaka (1973) introduced the concept of matrix average stress and developed an analytical approach to evaluate the macroscopic constants of composites with randomly distributed fibers.

The Mori-Tanaka estimate is relatively well adapted to the situation where the volume fraction of fibers is significant and, consequently, the distance between the inclusions allows them to "feel" each other. Therefore, the relationship between the strain in the inclusion and the applied strain on the composite can be obtained by the average strain of the matrix.

The Mori-Tanaka estimate of the overall stiffness tensor of the composite can be written as:

$$\underset{\sim}{C}^{hom} = \left\langle \underset{\sim}{C} : \left(\underset{\sim}{I} + \underset{\sim}{P} : \delta\underset{\sim}{C}\right)\right\rangle : \left\langle \left(\underset{\sim}{I} + \underset{\sim}{P} : \delta\underset{\sim}{C}\right)^{-1}\right\rangle^{-1}. \tag{7}$$

with $\delta\underset{\sim}{C} = \underset{\sim}{C}^{I} - \underset{\sim}{C}^{0}$ and $\underset{\sim}{C}^{0}$ referring to the elasticity of the matrix, (concrete), and $\langle . \rangle$ denotes the average over the composite. Thus, by introducing the volume fraction of fibers, f, the above expression can also be written as:

$$C_{ijkl}^{hom} = \left[(1-f) C_{ijpq}^{0} + f \left\langle C_{ijnm}^{I} A_{mnpq} \right\rangle_{I} \right] \left[(1-f) I_{pqkl} + f \left\langle A_{pqkl} \right\rangle_{I} \right]^{-1}. \quad (8)$$

where $\langle . \rangle_{I}$ is the average over the inclusion.

2.3 Application to FRC

The determination of the macroscopic characteristics of the composite requires the preliminary representation of tensor A_{ijkl} in global coordinates, because only its expressions in local coordinates or in relation to their main axles are known (Mura, 1982). The local directions of a given inclusion are displayed in Fig. 2a. Since expression of C_{ijkl}^{hom} involves the calculation of average quantities, the shape and orientation of each fiber should be prescribed.

The shape of a fiber can be described by its aspect ratio. In a local coordinate, the fiber with ellipsoidal shape is described by $x'^{2}_{1}/a^{2} + x'^{2}_{2}/b^{2} + x'^{2}_{3}/c^{2} \leq 1$, where a, b, and c are the half-axis length of the ellipsoid along the x_1', x_2' and x_3' directions, respectively (Fig. 2a). The aspect ratios, α_b and α_c, are defined as

$$\alpha_a = a/c \text{ and } \alpha_b = b/c. \quad (9)$$

If $\alpha_a = \alpha_b = 1$, the inclusion is spherical. If $\alpha_a = \infty$ and $\alpha_b = 1$, the inclusion is a prolate. As commented before, the fiber geometry in this work is modeled as a prolate inclusion.

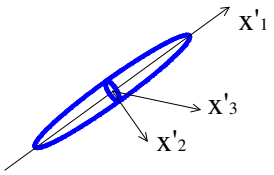


Figure 2a - Short fiber's local coordinates.

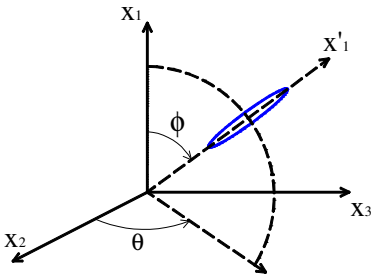


Figure 2b - Angles for fibers' orientation (Huang, 2001).

The fiber orientation can be described by means of two angles, θ and ϕ, as indicated in Fig. 2b. If X_{ijkl} and X'_{pqrs} represent the components of the same tensor, respectively in the local and global coordinate systems, the following relation holds.

$$X_{ijkl} = Q_{pi} Q_{qj} Q_{rk} Q_{sl} X'_{pqrs}. \quad (10)$$

where Q_{pi} are the components of the coordinate transformation matrix.

$$Q_{ij} = \begin{bmatrix} \cos\theta & \sin\theta\cos\phi & \sin\theta\sin\phi \\ -\sin\theta & \cos\theta\cos\phi & \cos\theta\sin\phi \\ 0 & \sin\phi & \cos\phi \end{bmatrix}. \quad (11)$$

Finally, the volume average over an inclusion can be obtained by the expression below. In this case, it is considered that the inclusions are of the same size.

$$\left\langle X_{ijkl} \right\rangle_I = \frac{1}{V_I} \int_{V_I} X_{ijkl} dV = \int_0^{2\pi} \int_0^{\pi} X_{ijkl}(\theta,\phi) \cdot p(\theta,\phi) \sin\theta d\theta d\phi . \tag{12}$$

where $p(\theta,\phi)$ is the density function of the fibers. In this study, $p(\theta,\phi) = 1/4\pi$, implying that the fibers are randomly orientated and distributed in all directions and regions of the composite. In such situation, the tensor of elastic properties, C_{ijkl}^{hom}, becomes isotropic and the bulk modulus, K^{hom}, and the shear modulus, G^{hom}, are obtained with the relations

$$\begin{aligned}
G^{hom} &= C_{1212}^{hom} = C_{1313}^{hom} = C_{2323}^{hom} \\
K^{hom} &= C_{1111}^{hom} - \frac{4}{3}G^{hom} = C_{2222}^{hom} - \frac{4}{3}G^{hom} = C_{3333}^{hom} - \frac{4}{3}G^{hom} \text{ or} \\
K^{hom} &= C_{1122}^{hom} - \frac{2}{3}G^{hom} = C_{1133}^{hom} - \frac{2}{3}G^{hom} = C_{2233}^{hom} - \frac{2}{3}G^{hom} .
\end{aligned} \tag{13}$$

3. RESULTS

The calculations were performed using the software Maple®. The obtained expressions are described below. It is recalled that these results correspond to the aspect ratios $\alpha_a = \infty$ and $\alpha_b = 1$.

$$K^{hom} = -\frac{3K^0G^0f + K^0G^If - 3K^IG^0f - K^IG^If - 3K^0G^0 - K^0G^I - 3K^0K^I}{3K^0f - 3K^If + 3G^0 + 3K^I + G^I} \tag{14}$$

$$G^{hom} = \frac{-(n_0 + n_1 + n_2 + n_3 + n_4 + n_5)}{d_0 + d_1 + d_2 + d_3 + d_4} \tag{15}$$

$$\begin{aligned}
n_0 &= -9fK^0\left(G^I\right)^3 K^I , \qquad n_1 = -3G^0\left(G^I\right)^2\left(5G^IK^0 + 7fG^IK^0 + 7fG^IK^I + 15fK^IK^0 + 15K^IK^0\right), \\
n_2 &= -\left(G^0\right)^2 G^I\left(35\left(G^I\right)^2 + 37f\left(G^I\right)^2 + 45fG^IK^0 + 105G^IK^I + 75G^IK^0 + 51fG^IK^I - 9fK^IK^0 + 90K^IK^0\right), \\
n_3 &= \left(G^0\right)^3\left(-145\left(G^I\right)^2 - 39f\left(G^I\right)^2 - 120G^IK^I - 45K^IK^0 - 105G^IK^0 + 45fK^0K^I + 57fG^IK^I + 21fG^IK^0\right), \\
n_4 &= \left(G^0\right)^4\left(-45K^0 - 15K^I - 125G^I + 61fG^I + 15fK^I + 45fK^0\right) \quad \text{and} \quad n_5 = 15\left(G^0\right)^5(f-1)
\end{aligned} \tag{16}$$

$$\begin{aligned}
d_0 &= -3\left(G^I\right)^2 K^0\left(-5G^I + 5fG^I + 12fK^I - 15K^I\right), \\
d_1 &= -G^0G^I\left(-35\left(G^I\right)^2 + 35f\left(G^I\right)^2 - 105G^IK^I + 84fG^IK^I + 39fG^IK^0 - 75G^IK^0 - 90K^IK^0\right), \\
d_2 &= \left(G^0\right)^2\left(145\left(G^I\right)^2 + 36fG^IK^I + 36fK^0K^I + 15fG^IK^0 - 73f\left(G^I\right)^2 + 45K^IK^0 + 105G^IK^0 + 120G^IK^1\right), \\
d_3 &= \left(G^0\right)^3\left(45K^0 + 125G^I + 15K^I + 48fK^I + 59fG^I + 39fK^0\right) \quad \text{and} \quad d_4 = \left(G^0\right)^4(15 + 49f) .
\end{aligned} \tag{17}$$

In order to analyze how the volume fraction and the properties of the constituents affect the elastic properties of the composite, the results corresponding to a concrete matrix and different types of fibers (steel, aramid, carbon, polypropylene, glass) are plotted in Fig. 3a and 3b. The elastic properties of the considered materials are detailed in the table below.

Table 1. Features of concrete and different types of fibers

Fiber	Poisson's ratio (ν)	Young's Modulus (E) (MPa)	Bulk Modulus (K) (MPa)	Shear Modulus (G) (MPa)
Steel	0.30	210000	175000	80769.23
Aramid	0.35	62000	68888.9	22963
Carbon	0.20	380000	211111.1	158333.3
Polypropilene	0.30	4000	3333.3	1538.5
Glass AR	0.22	80000	47619	32786.9
Concrete matrix	0.20	31000	17222.2	12916.7

In Figures 3a and 3b are displayed how the bulk and shear moduli vary with the volume fraction of fibers added. When no fiber is added (f=0), the values of these moduli correspond to the moduli of concrete matrix ($K^{hom}/K^0 = 1$ in Fig. 3a, and $G^{hom}/G^0 = 1$ in Fig. 3b). With the increasing addition of fibers, K^{hom} and G^{hom} increase or decrease depending on the values of the bulk and the shear moduli of the inclusion material.

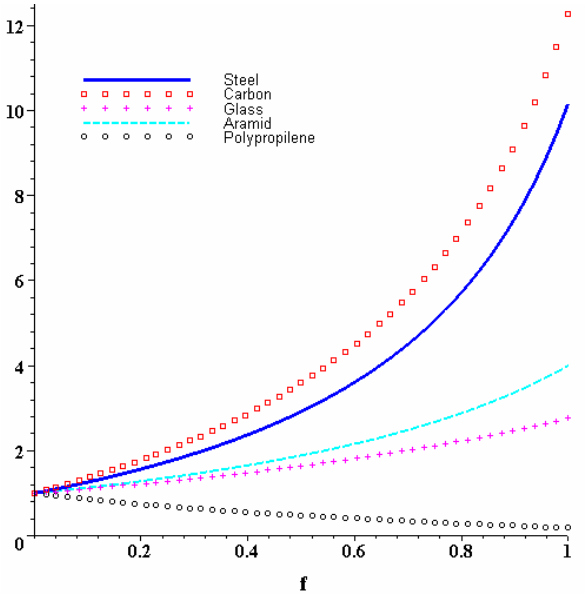


Figure 3a - Range of K^{hom}/K^0 according to the volume fraction of different types of fibers.

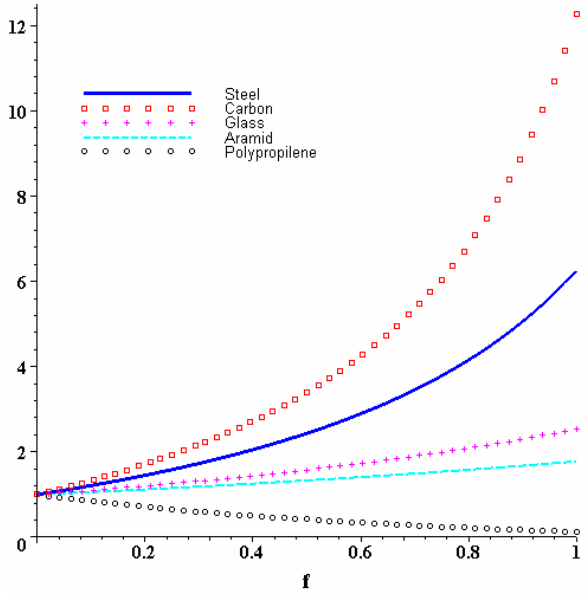


Figure 3b - Range of G^{hom}/G^0 according to the volume fraction of different types of fibers.

These results differ from those obtained using the simple mixture rule, where the elastic properties of composites are directly proportional to the properties of their constituents and the volume fraction of fibers ($K^{hom} = fK^I + (1-f)K^0$). Figure 4 shows the difference found between the results of the mixture rule and Theory of Homogenization through the estimate of Mori-Tanaka for concretes reinforced with steel fibers. The Figure indicates that the mixture rule may significantly overestimate the value of the elastic constant K of the composite.

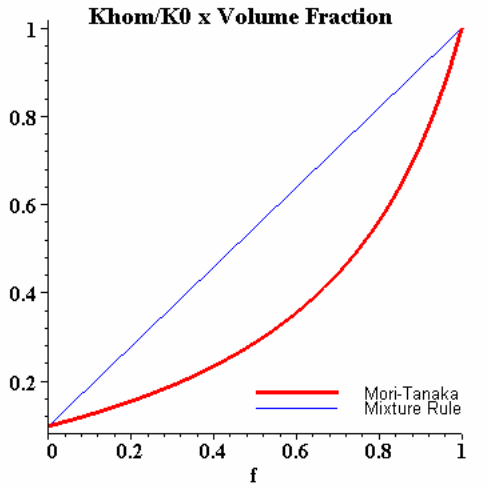


Figure 4 - Comparison between the Averaging Rule and the Estimate of Mori-Tanaka.

In order to verify the influence of fiber' aspect ratio, α_a, the problem is solved in a similar way to that previously described. The values adopted for α_a were 10, 40, 80, 100, and ∞, typical values for steel fibers. The results given in Fig. 5 correspond to the concrete matrix and steel fibers. Clearly enough, the value of the aspect ratio has a small influence on the elastic properties of the composite. This result is consistent with previous works available in the literature (Thomas and Ramaswamy, 2007; Ashour, 2000, Atiş and Karahan, 2007).

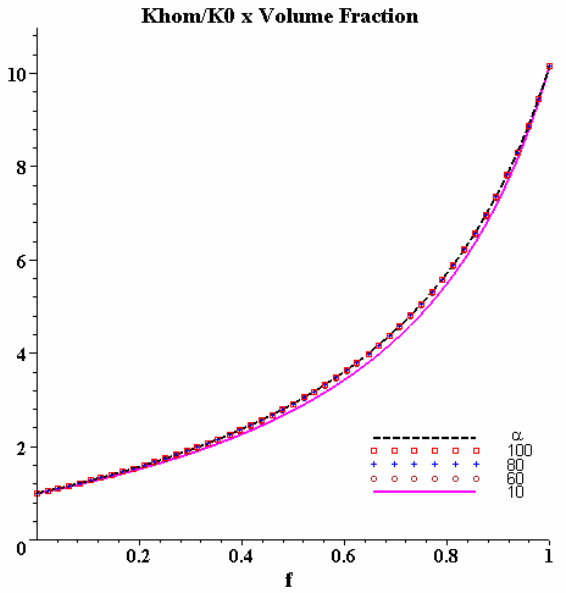


Figure 5a - Range of K^{hom}/K^0 according to the volume fraction for different values of α_a.

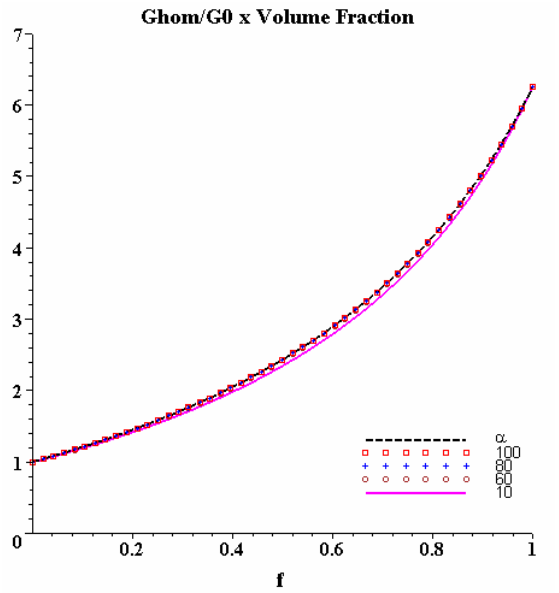


Figure 5b - Range of G^{hom}/G^0 according to the volume fraction for different values of α_a.

4. FINITE ELEMT ANALYSIS

In the analysis using the finite element method (FEM), the behavior of the composite material (FRC) is simulated by modeling the fibers as embedded bars in hexahedral finite elements of concrete. The fibers were considered as short segments of material with specific properties and randomly distributed in the elements of concrete. Figure 6 illustrates the fibers' arrangement.

The formulation adopted (embedded model) admits that the location and geometry of the fibers are independent of the finite element mesh, i.e., the nodes of the fiber elements do not need to be coincident with the nodes of the mesh. This allows the fibers to be placed in any location in the problem domain. The nodal displacements of fibers, in its turn, are written according to the nodal displacements of their respective elements of concrete. In this way, the fibers act as stiffeners, increasing the total stiffness of the reinforced media. In a finite element numerical approximation, this means that the fiber will be contributing to the stiffness of the element (or elements) in which it is embedded. Thus, the stiffness matrix of the reinforced media is composed by the stiffness matrices of the finite elements of concrete and of the finite elements of the embedded fibers.

The random distribution of fibers used allowed the modeling of each fiber as it is presented in real structures. The initial coordinates and director co-sines of fibers, which define the fibers' orientation in the three-dimensional space, are randomly generated in the program code (written in FORTRAN language). The final coordinates are determined by the initial coordinates, the director co-sines and the specified length of the fibers (Pasa, 2007).

A number of tests were conducted in order to compare the results obtained with the FEM modeling, and the micromechanics estimations described in the previous item. In these tests, fibers of 30 mm in length were embedded into a concrete cube of 100 mm of edge (only one finite element), and a concrete cube of 200 mm of edge (eight finite elements). Figure 6 illustrates the finite elements of concrete and the embedded fibers.

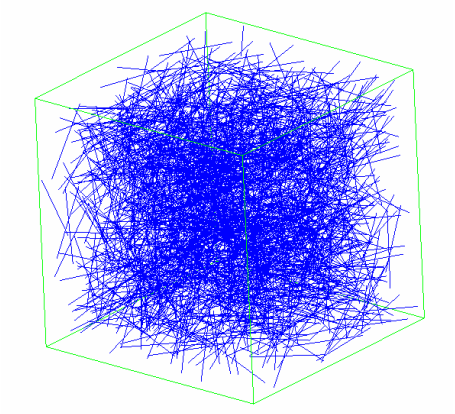


Figure 6a- $\alpha_a = 40$, f = 3% and 1 finite element.

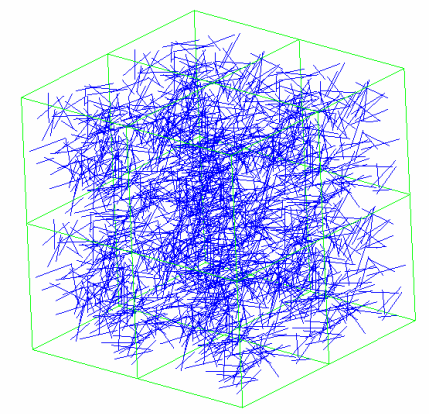


Figure 6b - $\alpha_a = 40$, f = 3% and 8 finite elements.

The material used for the fibers was the steel described in Table 1, where the properties of the concrete's matrix can also be found. The values adopted for the aspect ratios, α_a, and for the volume fractions were 10, 40, 80, and 100 and 3%, 5% and 10%, respectively. For cubes of 100 mm, different fiber arrangements were also tested through 8 modeling with different random distributions and the same amount and shape of fibers.

Table 2 exhibits the results: the averages of the Young's Modulus and the Poisson's ratio, the standard deviations (SD) and the coefficients of variation (CV) of the simulations of the

cubes of 100 mm (only one finite element). Table 2 also presents the results for the modeling of the cubes with 200 mm.

Table 2. Results

α_a	f (%)	Mori-Tanaka		1 FE (100 mm)						8 FE (200 mm)	
				Young's Modulus			Poisson's Ratio				
		E (MPa)	ν	E (MPa)	SD	CV	ν	SP	CV	E (MPa)	ν
10	3	3279.51	0.203	3252.19	13.75	0.0042	0.209	0.0012	0.0059	3252.29	0.209
	5	3403.31	0.205	3363.14	14.80	0.0044	0.214	0.0013	0.0060	3363.62	0.214
	10	3728.34	0.209	3618.52	27.52	0.0076	0.222	0.0029	0.0132	3614.23	0.221
40	3	3293.72	0.203	3245.41	4.84	0.0015	0.209	0.0002	0.0011	3245.51	0.209
	5	3427.13	0.205	3353.86	5.46	0.0016	0.213	0.0004	0.0017	3353.91	0.213
	10	3776.65	0.210	3605.17	5.96	0.0017	0.223	0.0004	0.0019		
80	3	3295.24	0.203	3245.37	1.94	0.0006	0.209	0.0002	0.0009		
	5	3429.68	0.205	3354.28	1.98	0.0006	0.213	0.0001	0.0003		
	10	3781.83	0.210	3604.42	4.02	0.0011	0.223	0.0002	0.0009		
100	3	3295.46	0.203	3247.37	1.85	0.0006	0.209	0.0001	0.0005		
	5	3430.05	0.205	3353.88	1.94	0.0006	0.213	0.0002	0.0010		
	10	3782.58	0.210	3605.85	2.61	0.0007	0.223	0.0002	0.0009		

Table 2 shows that the results of the problem have very similar values when it is examined for eight and for only one finite element. Moreover, the low values of the coefficients of variation (CV) indicate sets of response fairly homogeneous. Finally, comparing the results obtained through the Mori-Tanaka estimate and those obtained through computational simulations based on the finite element method, it can be observed that the values are very close, considering typical volume fractions ($f < 10$).

5. CONCLUSIONS

The macroscopic properties of a composite material formed by a concrete matrix and scattered fibers (FRC) are controlled by the properties of their constituents. The purpose of this study was to verify how the properties of the constituents of the FRC, the geometry and the volume fraction of fibers affect the macroscopic properties.

The results show that the elastic properties in the composite are not directly proportional to the amount of fibers added and the elastic properties of their constituents. A comparative study showed how determinations derived from the mixture rule can overestimate significantly the properties of FRC, especially when the components have very different characteristics, such as concrete and steel fibers. Moreover, it has been verified that the aspect ratio, α_a, has little influence on the macroscopic elastic properties of the composite.

Finally, the analysis by the finite element method of fibers randomly distributed suggests that the results are very close to those obtained from the homogenization schemes that employ the estimate of Mori-Tanaka.

Acknowledgements

The authors thankfully appreciate the financial support provided by the *Conselho Nacional de Desenvolvimento Científico e Tecnológico*, CNPq, and the much needed computational resources provided by the *Centro de Mecânica Aplicada e Computacional*, CEMACOM.

REFERENCES

Ashour, S. A., Wafa, F. F., Kamal, M. I., 2000. Effect of the concrete compressive strength and tensile reinforcement ratio on the flexural behavior of fibrous concrete beams. *Engineering Structures*, vol. 22, n. 9, pp. 1145-1158.

Atiş, C. D., Karahan, O., 2007. Properties of steel fiber reinforced fly ash concrete. *Construction and Building Materials.*

Benveniste, Y., 1987. A new approach to the application of Mori–Tanaka's theory in composite materials. Mechanics of Materials, vol. 6, n. 2, pp. 147-157.

Chen, C. H., Cheng, C. H., 1996. Effective elastic moduli of misoriented short-fiber composites. *International Journal of Solids and Structures*. vol. 33, n. 17, pp. 2519-2539.

Chou, T.W., Nomura, S., Taya, M., 1980. A self-consistent approach to the elastic stiffness of short-fiber composites. *Journal of Composite Materials*, n. 14, pp. 178-188.

Christensen, R. M., Lo, K. H., 1979. Solutions for effective shear properties in three phase space and cylinder model. *Journal of the Mechanics and Physics of Solids.* vol. 27, n.4, pp. 315-330.

Eshelby, J. D., 1957. The determination of the elastic field of an ellipsoidal inclusion, and related problems. *Proceedings of the Royal Society of London A 241*. pp 376-396.

Figueiredo, A. D., 2005. Concreto com Fibras. *Concreto Ensino, Pesquisa e Realizações.* Ibracon, v. 2. São Paulo: Ipisis Gráfica e Editora. chap. 39, pp.1195-1225.

Furlan Jr., S., Hanai, J. B., 1997. Shear behavior of fiber reinforced concrete beams. *Cement and Concrete Composites*, vol. 19, n. 4, pp 359-366

Hashin, Z., 1968. Assessment of the self-consistent scheme approximation. Journal of Composite Materials. n. 2, pp. 284-300.

Huang, J. H., 2001. Some closed-form solutions for effective moduli of composites containing randomly oriented short fibers. *Materials Science and Engineering A 315*. n 15, pp 11-20.

Jiang, B., Liu, C., Zhang, C., Wang, B., Wang, Z., 2007. The effect of non-symmetric distribution of fiber orientation and aspect ratio on elastic properties of composites *Composites Part B: Engineering*, vol. 38, n. 1, pp. 24-34

Mori T., Tanaka K., 1973. Average stress in matrix and average elastic energy of materials with misfitting inclusions. *Acta Metall.* n 21, pp 571-574.

Mura, T., 1882. *Micromechanics of defects in solids.* Martinus Nijhoff. Dordrecht, The Netherlands.

Pasa, V. F., 2007. *Análise do Comportamento de Estruturas de Concreto Reforçado com Fibras de Aço via Método dos Elementos Finitos*. 2007. Dissertação (Mestrado) – Programa de Pós Graduação em Engenharia Civil, UFRGS, Porto Alegre.

Teng, T. L., Chu, Y. A., Chang, F.A., Chin, H.S., 2004. Calculating the elastic moduli of steel-fiber reinforced concrete using a dedicated empirical formula. *Computational Materials Science.* n 31, pp 337-346.

Thomas, J., Ramaswamy A., 2007. Mechanical properties of steel fiber-reinforced concrete. *Journal of Materials in Civil Engineering*, vol. 19, n. 5, pp. 385-392.

Russel, W. B., 1973. On the effective moduli of composite materials: effect of fiber length and geometry at dilute concentrations. *Journal of Applied Mathematics and Physics (ZAMP).* n. 24, pp 581-600.

Zollo, R. F., 1997. Fiber-reinforced concrete: an overview after 30 years of development. *Cement & Concrete Composites*, vol. 19, n. 2, pp. 107-122